

Paving the Way for Motor Imagery-Based Tele-Rehabilitation through a Fully Wearable {BCI} System

Original

Paving the Way for Motor Imagery-Based Tele-Rehabilitation through a Fully Wearable {BCI} System / Arpaia, P., Coyle, D., Esposito, A., Natalizio, A., Parvis, M., Pesola, M., Vallefuoco, E.. - In: SENSORS. - ISSN 1424-8220. - ELETTRONICO. - 23:13(2023). [10.3390/s23135836]

Availability:

This version is available at: 11583/2982763 since: 2023-10-05T07:06:12Z

Publisher:

MDPI

Published

DOI:10.3390/s23135836

Terms of use:

This article is made available under terms and conditions as specified in the corresponding bibliographic description in the repository

Publisher copyright

(Article begins on next page)

Paving the way for motor imagery-based tele-rehabilitation through a fully wearable BCI system

Pasquale Arpaia^{1,2,3}, Damien Coyle^{4,5}, Antonio Esposito², Angela Natalizio^{2,6}, Marco Parvis⁶, Marisa Pesola^{1,2}, and Ersilia Vallefuoco^{2,7}

- ¹ Department of Electrical Engineering and Information Technology (DIETI), Università degli Studi di Napoli Federico II, Naples, Italy;
- ² Augmented Reality for Health Monitoring Laboratory (ARHeMLab), Università degli Studi di Napoli Federico II, Naples, Italy;
- ³ Centro Interdipartimentale di Ricerca in Management Sanitario e Innovazione in Sanità (CIRMIS), Università degli Studi di Napoli Federico II, Naples, Italy;
- ⁴ Institute for the Augmented Human, University of Bath, Bath, England;
- ⁵ Intelligent Systems Research centre, University of Ulster, Derry, Northern Ireland;
- ⁶ Department of Electronics and Telecommunications (DET), Politecnico di Torino, Turin, Italy;
- ⁷ Department of Psychology and Cognitive Science, University of Trento, Rovereto, Italy.
- † This paper is an extended version of our paper published in 2022 IEEE International Conference on Metrology for Extended Reality, Artificial Intelligence and Neural Engineering (MetroXRINE) (pp. 691-696). IEEE.

Abstract: The present study introduces a brain-computer interface designed and prototyped to be wearable and usable in daily life. Eight dry electroencephalographic sensors were adopted to acquire the brain activity associated with motor imagery. Multimodal feedback in extended reality was exploited to improve online detection of neurological phenomena. Twenty-seven healthy subjects used the proposed system in five sessions to investigate the effects of feedback on motor imagery. The sample was divided into two equal-sized groups: a "neurofeedback" group, which performed motor imagery while receiving feedback, and a "control" group, which performed motor imagery with no feedback. Questionnaires were administered to participants aiming to investigate the usability of the proposed system and individual's ability to imagine movements. The highest mean classification accuracy across subjects of control group was about 62 % with 3 % associated type A uncertainty, and 69 % with 3 % uncertainty for the neurofeedback group. Moreover, in some cases results were significantly higher for the neurofeedback group. The perceived usability by all participants was high. Overall, the study aimed at highlighting the advantages and the pitfalls of using a wearable brain-computer interface with dry sensors. Notably, this technology can be adopted for safe and economically viable tele-rehabilitation.

Keywords: electroencephalographic sensor; dry sensors; motor imagery; brain-computer interface; neurofeedback; tele-rehabilitation

Citation: Motor imagery-based brain-computer interface relying on dry sensors and neurofeedback: towards tele-rehabilitation. *Sensors* **2023**, *13*, 0. <https://doi.org/>

Received:
Revised:
Accepted:
Published:

Copyright: © 2023 by the author. Submitted to *Sensors* for possible open access publication under the terms and conditions of the Creative Commons Attribution (CC BY) license (<https://creativecommons.org/licenses/by/4.0/>).

1. Introduction

Tele-rehabilitation has long been considered a promising way of providing rehabilitative therapies "at distance" [1–3]. Digital sensing and artificial intelligence solutions enable patient-centered treatment by continuously monitoring and evaluating patient performances [4,5]. Over the past few years, the COVID-19 pandemic has accelerated this transition to a new era known as health 5.0 [6,7]. In this context, extended reality helped to provide an alternative therapy at a distance for a wide range of people. Notably, different solutions were proposed for older adults with neurodegenerative diseases [8–10].

Brain-computer interfaces (BCI) based on the motor imagery paradigm have been extensively studied for human patients with a variety of neuromuscular disorders in order to facilitate recovery of neural functions. Its effectiveness is confirmed especially for stroke

patients [11–13]. The combination of BCIs and extended reality can provide patients with neurofeedback on their mental tasks [14]. In particular, sensory feedback helps them in the self-regulation of brain rhythms and promotes neural plasticity.

Literature has shown that neurofeedback improves classification for motor imagery, and that sensorimotor cortical activation is significantly enhanced. This was quantified in terms of classification accuracy, with improvement of about 10 % to 20 % [15,16], but also as event-related spectral perturbation and functional connectivity [15].

To be involved in tele-rehabilitation, a system including BCI and extended reality must be non-invasive, wearable, portable, comfortable, and generally ready for getting out of controlled lab environments [17,18]. Moreover, wireless features are desirable in disclosing new applications with brain-type communication services [19]. These requirements are often fulfilled by exploiting electroencephalography (EEG) to acquire brain signals [20]. EEG systems for "out-of-lab" acquisitions are increasingly being developed [21]. These are mainly wireless devices with a reduced number of sensors that allow freedom of movement and improve usability [22,23]. Moreover, instead of the standard wet sensors, dry sensing could be used to increase user comfort while attempting to keep high metrological performance [24–26].

Previous studies already proposed EEG devices relying on dry sensors. They relied either on ad-hoc instrumentation [27–29] or evaluated consumer-grade instrumentation [30,31] involving dry electrodes. For instance, in [32], classification was attempted in different dry sensing setups (from 8 to 32 sensors) and with different signal processing approaches. A wireless high-density EEG medical grade system was used and a drop in performance was observed when 8 channels were used. However, neurofeedback was not investigated in trying to enhance motor imagery detection. Recently, the feasibility of a wearable BCI for neurorehabilitation at home was proposed in [33]. Healthy participants received remote instructions on the use of an EEG device with 16 dry sensors. Visual feedback consisted of a bar fluctuating vertically up or down from the midline. Half of the participants succeeded in controlling the BCI during six sessions.

It is worth noting that a previously published work [16] already investigated a similar motor imagery-based BCI with wet sensors. Moreover, unimodal feedbacks (visual and haptic) were investigated along with multimodal visual-haptic feedback. The results highlighted the role of neurofeedback in improving the performance, and participants generally preferred visual and visual-haptic feedback modality. Nonetheless, the experiments had to be extended to a greater number of participants.

The aim of present study was to prototype and validate a user-friendly BCI that could be then addressed to tele-rehabilitation. This was done by emphasizing wearability, comfort, engagement, and ease of use. An upgraded version of a previously proposed system [16] was designed and developed incorporating a ready-to-use Class IIA EEG device with 8 dry sensors, certified according to the Medical Device Regulation. The effectiveness of visual-haptic neurofeedback in discriminating between left hand and right hand motor imagery was also investigated over 5 experimental sessions for each of the 27 enrolled subjects. Notably, this multimodal feedback was chosen in accordance with the subjects' preference proven by the previous study [16]. To this aim, the subjects were divided into a control group and a neurofeedback group. Preliminary results were presented in [34], but extended here by considering a large subject cohort and results of questionnaires administered to evaluate usability. The remainder of the paper is organized as follows: Section 2 presents an overview of the proposed system, with a focus on the experimental protocol and outcome measures; Section 3 shows system performance in experiments; Section 4 concludes the manuscript by discussing the results.

2. Materials and methods

This section discusses the design, implementation, and validation methods for a wearable BCI relying on motor imagery, EEG with dry sensors, and online neurofeedback. An overview of the system is given together with adopted hardware. Then, EEG

processing is focused in association with the experimental protocol. Questionnaires will also be introduced. They were adopted to assess the usability of the system and imaginative abilities of its users. Finally, the tests considered within the statistical analysis are recalled.

2.1. System overview

The present study proposes a new system integrating a BCI with neurofeedback in extended reality, where a virtual reality environment was set to provide both visual and haptic virtual sensations (Fig. 1). This could be addressed both to daily-life applications for tele-operating a device [19,35] and to tele-rehabilitation purposes.



Figure 1. A subject using the proposed BCI system with neurofeedback in extended reality. The system involves EEG acquisition with the *Helmate* device, online processing, and actuators for visual-haptic feedback delivering.

In the system, brain signals were acquired by using the *Helmate* EEG device by *abmedica*¹. This is a Class IIA device certified according to the Medical Device Regulation (EU) 2017/745. It has eight measuring channels plus one reference channel and one bias channel. Ten dry sensors with different shapes can be chosen according to the zone of the scalp to reach. Moreover, as a multipurpose device, different configurations for the channels' location could be exploited. In this study, the eight measuring channels were located at FP1, FP2, Fz, Cz, C3, C4, O1, and O2 according to one of the default configurations, while the reference and bias sensors were placed in the frontal region at AFz and FPz, respectively (Fig. 2). Such a configuration guarantees optimal mechanical stability of the helmet during measurements. Moreover, it makes the system open to future upgrades by allowing, for instance, the integration of a module for monitoring users' engagement.

Data were collected at a sampling rate of 512Sa/s and transmitted via Bluetooth to a custom Simulink model for EEG processing. In Simulink, features from the EEG signal were extracted by means of the filter bank common spatial pattern (FBCSP) [36] and classified by means of the naive Bayesian Parzen window (NBPW). The latter returns two outputs: the class to which the multi-channel EEG signal is assigned (right or left), and the probability associated with that class.

The classification outputs were used to drive multimodal feedback through a custom Unity application. The neurofeedback consisted of a combination of visual and haptic feedback associated with mind-control of a virtual object and coherent tactile sensation. For visual feedback, a virtual ball was shown on a display (Fig. 3). This could roll to the left or to the right of the virtual environment according to the EEG classification. In detail,

¹ <https://www.abmedica.it/>

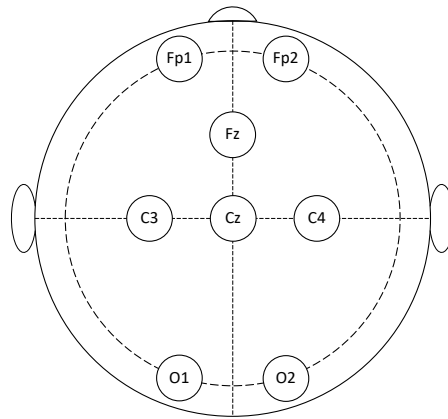


Figure 2. Position on the scalp of the sensors adopted in this study. Locations are identified by the 10-20 standard system for EEG.

while the assigned class determined the direction, the related score determined its velocity. The TactSuit X40 from bHaptics Inc was instead used for the haptic feedback. This is a wearable and portable vest equipped with 40 individually controllable vibrotactile motors. The vibration was again modulated by classification outputs. More specifically, the pattern could move from the center of the torso (front side) to the right or to the left in accordance with the assigned class. Meanwhile, the related score determined the vibration intensity. It is worth noting that the only bottom motors were used to minimize vibration artifacts on the EEG signals.

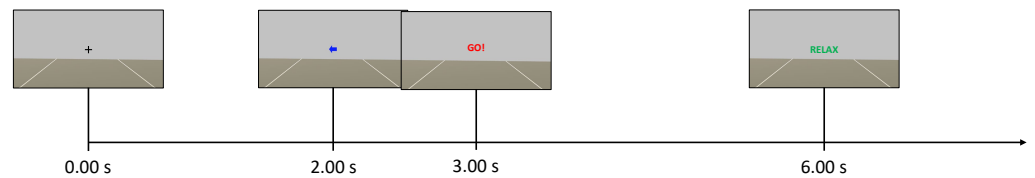


Figure 3. Timing of a single trial of the experimental sessions for the control group. The same timing was also used for the neurofeedback group during the only first phase of an experimental session. Notably, there was an overlap of 0.25 s between the cue and the word "GO!".

2.2. Experimental protocol

The described BCI was exploited within a cue-based (synchronous) paradigm. This implied that the user had to imagine a movement or be relaxed in accordance with given indications (the cues). The indications were delivered visually by means of the Unity3D platform. Two motor imagery tasks were possible, namely imagining the movement of the left hand or imagining the movement of the right hand. In case of neurofeedback, multimodal feedback was delivered to the user in response to the ongoing mental task. It should be noted that this was not simply intended for training the user (i.e., neurofeedback training), but as a part of the BCI online operation. Indeed, the actual role of this neurofeedback was to enhance the users' experience by providing some information on the ongoing brain activity. On the other side, the classifier adopted for the online processing had to be identified. This was done by exploiting signals acquired during pure motor imagery (no feedback).

In the experimental protocol, subjects were divided into two groups and involved in five one-hour experimental sessions over five weeks. The subjects assigned to a *control group* never received feedback. Instead, for the subjects of the *neurofeedback group*, pure mo-

tor imagery had to be recorded at the beginning of each session, and then neurofeedback was provided thanks to an EEG classifier trained on these preliminary data. The protocol for the two groups is described in detail in the following.

2.2.1. Control group

The Unity application dictated the timing within the experimental session. A total of six runs were recorded, and each run consisted of 30 trials. Each trial consisted of a fixation cross visualized from 0.00 s to 2.00 s, a cue (left or right arrow) visualized from 2.00 s to 3.25 s, the word "GO!" visualized from 3.00 s to 6.00 s, and the word "RELAX" visualized for a random time window of 1.00 s to 2.00 s (Fig. 3). Notably, words were displayed to guide the user through the experiment in the absence of any feedback on the screen. The sequence of left and right cues and the duration of the final "RELAX" were randomized across trials to avoid biases. The EEG was acquired as a continuous stream during each run, but never processed online and thus the control group did not receive any feedback. The runs were separated by short breaks, with a longer time break between the first three runs (phase 1) and the last three runs (phase 2) of a session.

2.2.2. Neurofeedback group

The first three runs of each session (phase 1) were carried out as done for the control group. However, during the time break between the phases, the EEG data from phase 1 were used to train the online classifier. This classifier was trained from scratch for each subject and for each session. Subsequently, participants of this group performed three further runs (phase 2) during which they received online multimodal feedback in response to motor imagery. The goal of the participants in the neurofeedback group was to move the visual feedback ball over the white lines of the game environment and to maximally activate the motors of the vest on the back of the respective side (i.e., left or right). In this experimental phase, words were no longer appearing but the user was fully guided by the arrows and the virtual ball (Fig. 4). In this case, the timing was slightly changed because participants were asked to start imagining from the appearance of the cue at $t = 2.00$ s. Then, they received the feedback from 4.50 s to 6.00 s (Fig. 4). The instant $t = 4.50$ s depended on the fact that the system actually started to classify at $t = 2.50$ s, and the time window for online processing was 2.00 s wide. Finally, the feedback could only move if the label obtained from the online classifier matched the assigned task (positive bias). Otherwise, no feedback was provided and the virtual ball was dragged towards the center of the screen while the intensity of the vibration was interrupted. Further details on that are discussed in the next subsection.

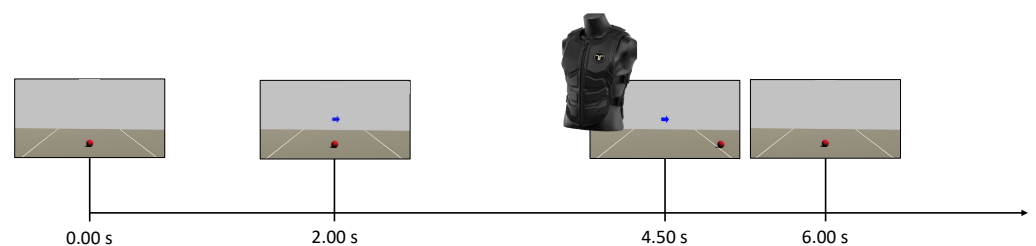


Figure 4. Timing of a single trial of the experimental sessions for phase 2 of the neurofeedback group. Instead, the same timing of the control group was used for phase 1.

2.3. EEG processing

The FBCSP with the NBPW classifier were used not only for online processing, but also for offline processing of EEG data. This is a well-known approach in the literature of motor imagery BCI [36] and it is still considered as one of the most successful ones for binary classification [37]. Its main blocks involve:

1. time domain filtering by means of a filter bank (FB) with 17 overlapped bandpass Type II Chebyshev filters with order 10 from 4 Hz to 40 Hz;
2. features extraction using a spatial domain filtering by means of the common spatial patterns (CSP) algorithm [35];
3. feature selection based on the class-related information content of the features by using the mutual information-based best individual features selector;
4. feature classification exploiting the Bayesian (NBPW) classifier.

Further details on the processing pipeline can be found in [16,34,36]. With reference to the neurofeedback group, after acquiring the EEG in a first half-session, data processing was needed to train the online classification algorithm. Specifically for online processing, the FBCSP-based approach was adapted so that the EEG stream was processed with a sliding window covering the motor imagery period.

By exploiting the results of previous studies [16,34], the time-width for the sliding windows was fixed at 2.00 s, and this was used to span the interval from 0.00 s to 7.00 s with a 0.25 s shift. A five-folds cross validation with five repetitions was used to identify the best portion of the EEG trials for training the algorithm. This best 2.00 s-wide window was selected as the one associated with the highest mean classification accuracy and the lowest difference between classification accuracies per class. Possible windows were extracted from the motor imagery window by considering all trials of phase 1.

Finally, at the end of the experiments, all data were processed offline to classify all data and assess the related accuracy. Differently from above, an artifact removal technique was introduced as a pre-processing step preceding the processing pipeline discussed above. This consisted of the artifact subspace reconstruction (ASR) technique, which was applied to raw signal during offline processing [38]. This is a relatively recent technique for artifact removal exploited here to prepare data prior to feature extraction and classification. ASR uses an artifact-free data segment as a baseline and then corrects the original data by calculating a covariance matrix and retrieving statistics to identify and remove artifacts. Notably, its usefulness for an eight EEG channels setup is supported by previous studies [39].

The ASR was applied by means of EEGLAB, a MATLAB© open-source toolbox for EEG analysis developed by Delorme and Makeig in 2004 [40]. Notably, the plug-in for cleaning raw data was specifically used.

2.4. Outcome measures

To evaluate the usability of the proposed system and the participants' imaginative abilities, the following questionnaires were administered to participants of both groups:

- MIQ-3 [41]: this is the most recent version of the movement imagery questionnaire [42] and of the movement imagery questionnaire-revised [43]. It is a 12-item questionnaire to assess an individual's ability to imagine four movements using internal visual imagery, external visual imagery, and kinaesthetic imagery. The rating scales range from 1 (very difficult to see/feel) to 7 (very easy to see/feel). The MIQ-3 has good psychometric properties, internal reliability and predictive validity.
- SUS (system usability scale) [44]: this is one of the most robust and tested psychometric tools for user-perceived usability. The SUS score consists of a value between 0 and 100, with high values indicating better usability. According to Bargar et al. [45], it is possible to adopt a 7-point adjectival scale (from "worst imaginable" to "best imaginable") for the SUS score. Another variation, proposed in [46], is to consider the score in terms of "acceptable" (value above 70) or "not acceptable" (value below 50). The range from 50 to 70 is instead "marginally acceptable".
- NASA-TLX (acronym for NASA task load index) [47]: it is a subjective, multidimensional evaluation tool that assesses perceived workload while performing a task or an activity. The original version also includes a weighting scheme to account for individual differences. However, the most common change made to the questionnaire is

the elimination of these weights in order to simplify its application [48]. In this work, it was administered without weights.

- UEQ-S (user experience questionnaire-short form) [49]: a standardized questionnaire to measure the user experience of interactive products. It distinguishes between pragmatic and hedonic quality aspects. The first describes interaction qualities that relate to tasks or goals the user wants to achieve when using the product. The second describes aspects related to pleasure or enjoyment while using the product. Values between -0.8 and $+0.8$ represent a neutral evaluation of the corresponding scale, values greater than $+0.8$ represent a positive evaluation, while values lower than -0.8 represent a negative evaluation.

The MIQ-3 was administered twice: before the first experimental session and at the end of the last experimental session. On the contrary, the other questionnaires were administered only at the end of the experimental sessions. In addition, during each experimental session, the participants were also given a short interview to assess their physical and mental state. This interview was adapted from the questionnaire proposed in [50], with some modifications needed to introduce aspects associated with neurofeedback [16].

2.5. Statistical Analysis

To compare classification accuracies between sessions and groups, a repeated-measures ANOVA test was used under the assumption of normally distributed data and homoscedasticity. The Jarque-Bera test was exploited to check for the normality assumption. Instead, the homoscedasticity was tested by means of the Bartlett's test. In case of a violation for the assumption of homoscedasticity, it was possible to apply a Welch's correction before applying the ANOVA. Meanwhile, when data were not normally distributed, the Kruskal-Wallis non-parametric test was used instead of the ANOVA.

The comparison of MIQ-3 scores between the two groups and the two endpoints (before starting and at the end of the sessions) was conducted via the Mann-Whitney-U-Test [51]. In addition, a Wilcoxon signed-rank test was used to compare paired data of the MIQ-3 scale within each group (control and neurofeedback). Similarly, a comparison between the two groups was carried on in terms of SUS, NASA-TLX, and UEQ-S scores at the end of the sessions. In each case, test-specific assumptions were checked before applying the test.

The statistical analyses were performed by using MATLAB (version 2021b) and the significance level for them was set by $\alpha = 5\%$ (probability of a false negative, or type-I error).

3. Results

Results are reported in this section after commenting on the sample of participants to the experimental campaign. Experimental data were analyzed in accordance with the methods of Section 2. Then, classification accuracies were exploited to assess the performance of the system and to describe its limits. Neurophysiological changes were also evaluated for each subject. The results are discussed in conjunction with answers to the questionnaires especially to address the usability of the system in tele-rehabilitation.

3.1. Participants

A sample of 27 healthy volunteers were enrolled in the study (mean age: 26, standard deviation: 2). The study was approved by the Ethical Committee of Psychological Research of the Department of Humanities of the University of Naples Federico II, and all the participants provided a written informed consent before starting the experiments.

To investigate multimodal feedback, roughly half of the participants were assigned to the "control group" and half to the "neurofeedback group". The two groups were balanced by age. In the control group, four subjects were males and nine were females. Meanwhile, in the neurofeedback group, eight subjects were males and six were females. All participants used the wearable system with dry sensors while seated in front of a display

Table 1. Summary of participants information for control and neurofeedback groups. BCI experience: experience with brain-computer interfaces in active paradigms, passive paradigms, reactive paradigms, multiple paradigms, or no experience. NF experience: previous experience with neurofeedback, no experience.

	Control	Neurofeedback
sex	male: 31 %, female: 69 %	male: 57 %, female: 42 %
handedness	right: 85 %, left: 15 %, both: 0 %	right: 79 %, left: 14 %, both: 7 %
practicing sport	yes: 38 %, no: 62 %, professional: 0 %	yes: 64 %, no: 36 %, professional: 0 %
BCI experience	no: 38.5 %, active: 8 %, passive: 15 %, reactive: 0 %, multiple: 38.5 %	no: 43 %, active: 7 %, passive: 21 %, reactive: 0 %, multiple: 29 %
NF experience	yes: 46 %, no: 54 %	yes: 36 %, no: 64 %

for visual indications and eventual feedback. Participants with affected motor and/or cognitive functions were excluded. However, it is worth mentioning that a subject (C08) reported of past epileptic seizures during childhood.

Most subjects were right-handed with the exception of two left-handed subjects per each group and one ambidextrous subject in the neurofeedback group. More than 60 % of participants for the neurofeedback group practiced sport, while participants to the control group practicing sport were less than 40 %. No participant played sport at a professional level. More than 50 % of participants already had experienced some BCI paradigms, and some subjects also had previous experience with neurofeedback. Such information is detailed in Table 1 along with a summary of previous information about sex, handedness, and sport practicing.

3.2. System performance

Classification results are shown in Fig. 5 for the control group. The matrix on the left reports the classification accuracy obtained on the first three runs of pure motor imagery (phase 1) across five sessions (x-axis) and for the 13 subjects (y-axis). The matrix on the right reports the analogous results for the last three runs of pure motor imagery (phase 2). Higher classification accuracy is indicated by red color. Meanwhile, a white space refers to a missing result caused by corrupted data or skipped session.

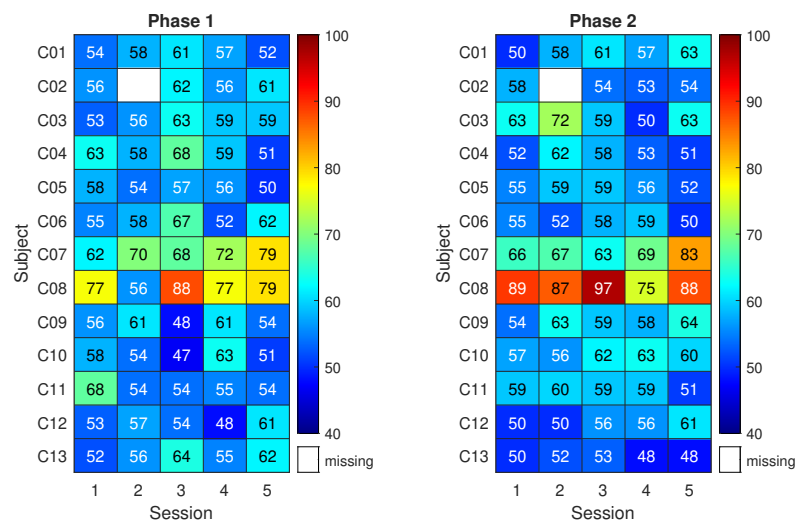


Figure 5. Control Group: mean classification accuracy using the best 2-seconds window.

Given that 90 trials were used for each classification result, the classification accuracy of a random classifier would be modeled by a binomial distribution with mean equal to 50 % (the well-known chance level) and a 95 % coverage interval spanning from 40 % to 59 % (related to the number of trials) [52]. Notably, this implies that only classification

accuracy values above 59 % can be considered non-random with an $\alpha = 5\%$. Therefore, for subjects in the control group, the classification accuracy resulted compatible with randomness except in a few cases. Overall, the highest mean classification accuracy across subjects was about 62 % with 3 % associated type A uncertainty and it was obtained either in phase 2 of session 2 and phase 1 of session 3.

Only subjects C07 and C08 do not belong to the general trend. Notably, the classification accuracies exceed 70 % in several cases, an empirical threshold for acceptable performance in motor imagery. Interestingly, C08 was the participant reporting past epileptic seizures.

On the other hand, Fig. 6 shows the classification results for the neurofeedback group. The matrix on the right refers to three runs with neurofeedback (phase 2 for the neurofeedback group). The results of phase 1 for the neurofeedback group appear similar to those

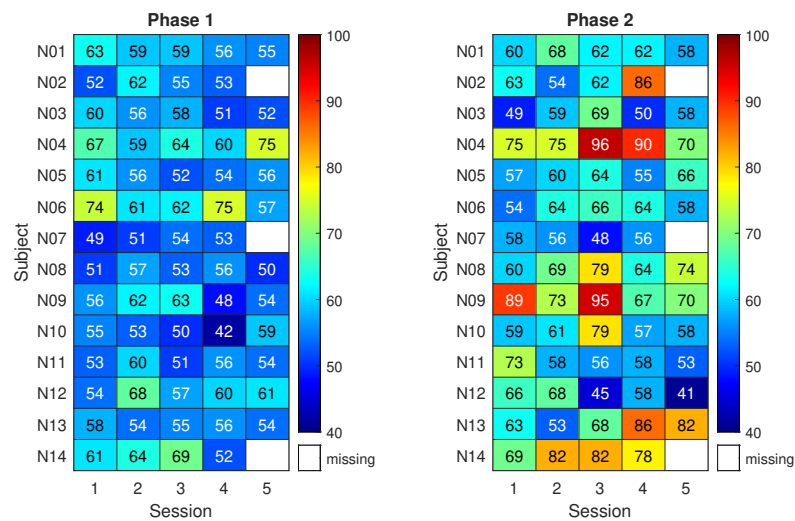


Figure 6. Neurofeedback Group: mean classification accuracy using the best 2-seconds window.

of the control group, with classification accuracies close to the chance level. Nonetheless, during phase 2, eight subjects out of 14 exceeded the 70 % accuracy threshold at least once. In more detail, by individually considering the sessions, the average improvement in classification accuracy due to neurofeedback ranges from 5 % to 12 %. The subjects reached the respective peak accuracy in different sessions. This led to a maximum average classification accuracy among subjects of 69 % with 3 % uncertainty.

Statistical testing suggested that the highest classification performance of the neurofeedback group in phase 2 does not differ significantly from the highest of the control group, though it is 7 % higher on average. Instead, a statistically significant difference between the two groups was found when focusing on the third session of phase 2 ($p < 0.05$). Moreover, classification accuracy in phase 2 resulted significantly higher than that of phase 1 in the fourth session of the neurofeedback group ($p < 0.005$). Finally, when comparing all the classification accuracies (all subjects and all sessions) of the neurofeedback group with those of the control group, the improvement given by neurofeedback in phase 2 is statistically significant ($p < 0.005$).

3.3. Questionnaires

As mentioned in Section 2, the MIQ-3 was administered twice to each subject, i.e., before the first and at the end of the experimental sessions. In the scale from 1 to 7, the mean scores resulted above 5 already at the first endpoint, with the only exception of kinesthetic imagery, whose mean score equaled 4 for both groups. This implies that subjects generally considered easy, or at least not difficult, to see/feel the involved movements. The Wilcoxon signed-rank test did not produce statistically significant variations in MIQ-3 paired scores, within each group. The same applies to the Mann-Whitney-U-Test when considering differences between the two groups before and after the experiments.

On the other hand, the SUS scores suggest that the system was considered acceptable by both groups (above 70). Specifically, the results are equal to 78 ± 10 and 75 ± 11 for control and neurofeedback groups, respectively. In addition, the overall results of the UEQ-s equaled 1.60 ± 0.64 for the control group and 1.70 ± 0.80 for the neurofeedback group. No statistically significant differences between the groups were detected ($p = 0.40$ for SUS and $p = 0.98$ for UEQ-s).

Finally, the NASA-TLX results are reported in Fig. 7. This shows similar subscales results for both groups with the exception of the effort. In particular, for the latter dimension, the Mann-Whitney-U-Test found statistically significant differences between the two groups ($p < 0.05$) indicating that the neurofeedback group perceived that there was more effort required than the control group which was anticipated due to the need to engage with neurofeedback. The mental demand was high (around 75 for both groups), while the frustration level, the performance, as well as temporal and physical demand resulted low.

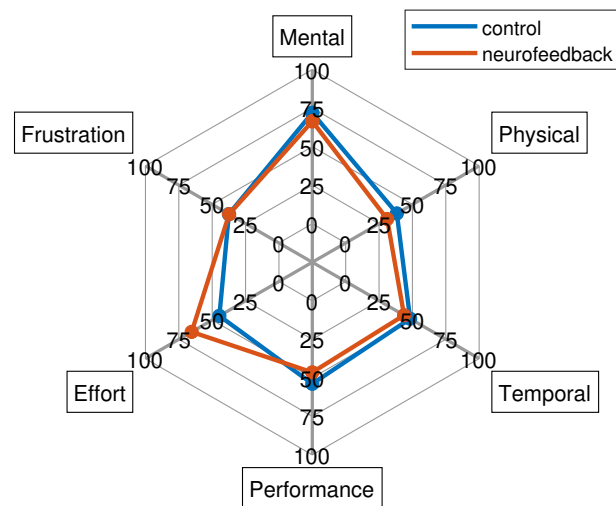


Figure 7. NASA-TLX results for both control and neurofeedback groups.

4. Discussion

In this concluding section, the results in terms of system performance and its acceptability by healthy users are thoughtfully discussed. Next, how the present work discloses the possibility of a tele-rehabilitation is commented on by relying on the current results to address future steps. Overall, both the limitations and strengths of the proposed system are considered in aiming to target the rehabilitation field.

4.1. System features and acceptability

Motor imagery-based BCIs present the possibility of novel rehabilitation paradigms, either substituting or supplementing current therapy protocols. This technology can be an option for safe and economically viable home-based therapies.

On the other hand, several training sessions are typically required to successfully control such a BCI and, as a well-known problem in literature, BCI illiteracy specifically prevents its widespread adoption. In such a framework, this study investigated the usage of neurofeedback to help a user to successfully control the system in few sessions while stressing daily-life and tele-rehabilitation requirements. As key aspects, the foreseen applications led to the adoption of a wearable and portable EEG with dry sensors, a wearable

and portable actuator for the haptic feedback, and an easy-to-use software application including the visual feedback.

Indeed, using the dry sensors increased the comfort for the participants mostly by avoiding the usage of conductive gels. However, the signal-to-noise ratio of the EEG data results generally lower than the one associated with wet sensors. This appeared especially true if the user had medium to long hair. For instance, when using dry sensors, EEG signals resulted as more affected by artifacts. The main artifacts superimposed on the EEG signal were heartbeats (especially at O1 and O2), breathing, ocular artifacts, and sweat artifacts (especially at F1 and F2). Furthermore, unlike wet sensors [16], vibration-induced artifacts occasionally appeared when the feedback was delivered by the haptic suit. Although ASR applied offline removed most artifacts, suit vibration had to be kept under control during online experiments, mostly by limiting its vibration intensity. On the other hand, this also suggests that a different type of haptic feedback should be explored in the future.

In the proposed system, feedback was implemented in a non-immersive extended reality by simultaneously providing multiple sensory stimulation, namely the haptic and visual modalities. With respect to unimodal feedback, a greater impact on classification performance was expected [16]. Moreover, the multi-sensory stimulation aimed to increase users' engagement. The resulting mean improvements (on the subjects) are in accordance with the previous evidence, which suggested that such feedback would have led to about 6% to 8% improvement in classification accuracy if compared to the absence of feedback. In particular, a 7% increase was highlighted between the control group and the neurofeedback group, while the mean improvement between the two phases for the neurofeedback group ranged from 5% to 12%. Therefore, although only 8 dry sensors were employed, the use of multimodal feedback led to an increase in system performance. In comparison, the subjects of the control group showed no significant improvement across the sessions, with the only exception of subjects C07 and C08, who achieved good results even without any feedback.

The results in terms of classification accuracy can be also supplemented with physiological information by neurophysiological changes. Notably, in accordance with the discussed literature, event-related spectral perturbation was investigated. To this aim, Fig. 8 reports time/frequency maps for the first session of subject N09 from the neurofeedback group. The figure focuses on the channels C3 and C4 in case of left hand imagery (Fig. 8a) and right hand imagery (Fig. 8b). The subject reached a low classification accuracy in this first session and, at the same time, there is only a desynchronization appearing in the beta band for the right hand motor imagery on C3, while the same phenomenon is not appearing for the left hand imagery.

Instead, Fig. 9 reports the time/frequency maps obtained in a different experimental session, in which the same subject reached the highest classification accuracy during neurofeedback (third session of N09). In such a case, and in accordance with literature [53,54], left-hand motor imagery is associated with a bilateral desynchronization (Fig. 9a) while right-hand motor imagery is associated with a contralateral desynchronization (Fig. 9b). Moreover, the timing of the event-related spectral perturbation is compatible with the best 2.00 s-wide window selected in calculating the classification accuracy. Notably, the best window for this subject in the third session was from 4.00 s to 6.00 s.

The time/frequency maps representative of the neurofeedback group were also compared with those of the subject C07 from the control group. In particular, this subject was taken into account because it reached one of the highest classification accuracies. For instance, with respect to the last experimental session, a contralateral desynchronization in the 10 Hz to 15 Hz band appears for left hand motor imagery (Fig. 10a) and a contralateral desynchronization also appears for right motor imagery (Fig. 10b). Notably, the best 2.00 s-wide window for this subject and for this session was 2.75 s to 4.75 s, where both neurophysiological phenomena occur.

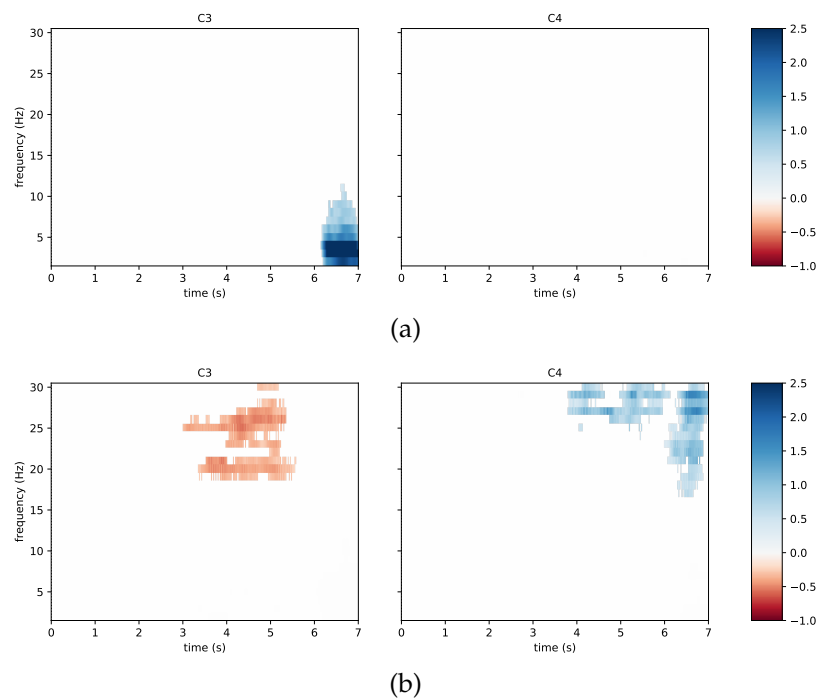


Figure 8. Time/frequency maps for a poorly performing subject from the neurofeedback group: (a) left hand imagery, (b) right hand imagery. The channels C3 and C4 are taken into account. Event-related desynchronization is depicted in red and event-related synchronization in blue.

With the short interview administered during each experimental session, it was also possible to monitor the subjects' mental and physical state during the sessions, as well as the type of imagined movement. In general, the most common imagined movements were squeezing a ball, moving the arm, tapping, grasping an object, dribbling, or playing piano. Nonetheless, it is worth noting that six out of 13 subjects in the control group changed the type of movement imagined during the sessions and, among these, three subjects also switched between internal, external, and kinaesthetic imagery. Seven out of 14 subjects in the neurofeedback group changed the type of imagined movement during the sessions and, also among these, four subjects changed between internal, external, and kinaesthetic imagery. According to the results, one can suspect that low-performance levels would also be also caused by changes in the imagined movement during the sessions, especially when feedback was not provided. Therefore, such an aspect should be more rigorously kept under control in future protocols.

Overall, SUS and UEQ-s questionnaires showed that the system is user-friendly, and subjects of both groups had a positive experience. This was not obvious with dry sensors because these require proper pressure to obtain a suitable electrode-skin contact. In turn, this could have implied pain and affected the overall system, whereas motor imagery requires deep users' concentration on the task. Contrary to expectations, the MIQ-3 did not show differences between groups and sessions as the imagination scores reported by the participants were high both before and after the experiments. A possible explanation would be that such a questionnaire is not directly linked to left/right hand movements, which are instead common motor imagery tasks. Therefore, its scale may be not sensitive enough for the tasks of this work, although no other standard scale exists for this purpose. Finally, the NASA-TLX effort was statistically higher for the neurofeedback group. This result may be explained by the constant demand required by these subjects, who received a response to their mental state during the online experiment.

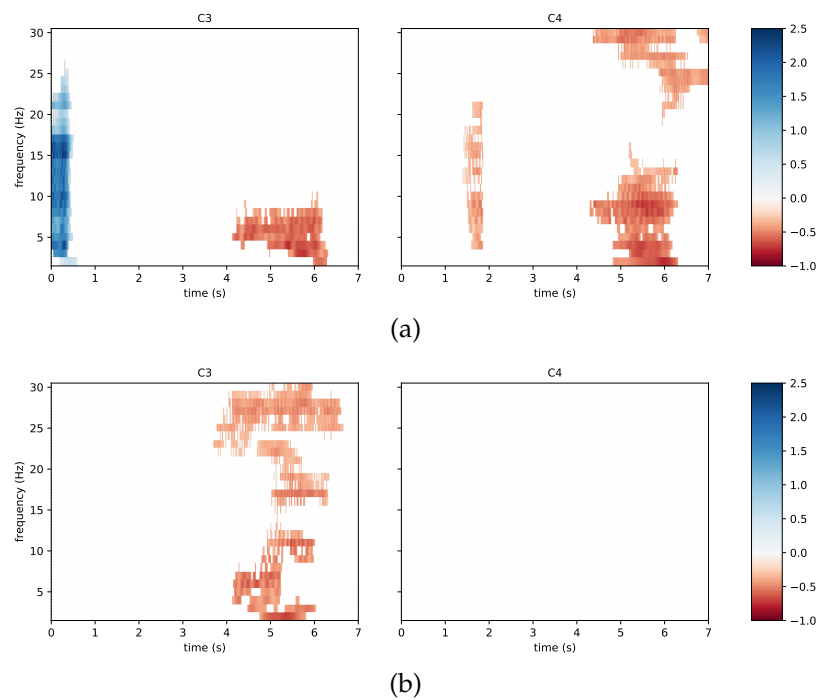


Figure 9. Time/frequency maps associated with the best accuracy result of the same subject from Fig. 8: (a) left hand imagery, (b) right hand imagery. The channels C3 and C4 are taken into account. Event-related desynchronization is depicted in red and event-related synchronization in blue.

4.2. Toward tele-rehabilitation

Several studies demonstrate the benefits of motor imagery-based systems for patients with variegated neurological diseases [55–57]. In these cases, neurophysiological signatures of motor imagery may undergo changes following brain trauma [58]. Indeed, such patients may present various medical conditions posing challenges for BCI-based tele-rehabilitation. These include cognitive impairment and different sensory deficits [59]. Moreover, it is crucial to recognize that, after lesions in the central nervous system, brain reorganization takes place. This can significantly impact the recovery of lost sensory and motor functions [55]. Therefore, the integration of motor imagery with neurofeedback assumes significance as an essential component of rehabilitation procedures. Another essential element should be considered in BCI-based tele-rehabilitation is considering the wide spectrum of needs of patients in terms of usability and applicability. Indeed, factors such as frustration, cognitive load, and fatigue can significantly impact the patients experience and their interaction with the system.

Despite its exploratory nature, this work offers valuable insights into BCI-based tele-rehabilitation. Firstly, the proposed system allows for home use thanks to its features, e.g., the dry electrodes employment. Using the system at home also discloses the possibility to reduce the duration of rehabilitation sessions while increasing their number. In addition, our results in mental fatigue can be useful to direct future therapy applications especially for patients with cognitive impairments. Finally, the present study suggested that animated objects or better limbs could aid in imaging movements. This aspect is essential for patients with motor disabilities, which may have more difficulties in maintaining vivid motor images with respects to healthy subjects [60,61]. The addressed improvements will be possible thanks to the wearability and the rehabilitation benefits of the proposed motor imagery-based BCI. Overall, the investigated system will be addressed tele-rehabilitation purposes because of the perceived usability and the substantial improvement in classification accuracy revealed in the neurofeedback group with respect to the control group.

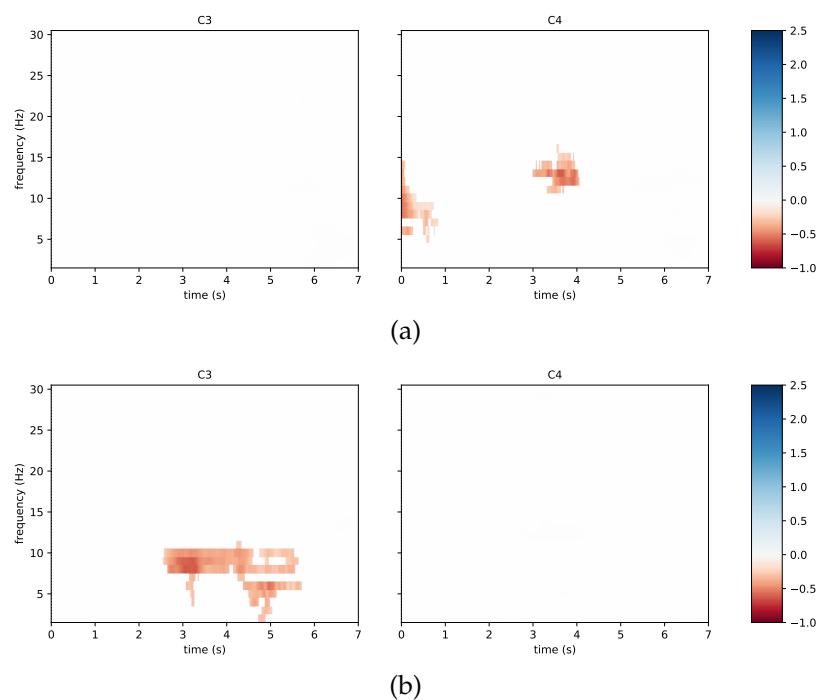


Figure 10. Time/frequency maps associated with a subject of the control group reaching high classification accuracy: (a) left hand imagery, (b) right hand imagery. The channels C3 and C4 are taken into account. Event-related desynchronization is depicted in red and event-related synchronization in blue.

A limitation of this study in tele-rehabilitation applications is that the multimodal proposed feedback was positively biased. Nonetheless, this can be enhanced with an adaptive bias to optimize system performance and patient learning [62], and future development could also focus on improving the classification algorithm to enhance performance across sessions and deliver better feedback [63]. Although multiple sessions were carried out already with healthy subjects, it is worth emphasizing patients would require even more training sessions to gain proper control over the BCI system and obtain benefits from therapy [64].

5. Supplementary material

The dataset is available at <https://metroxraine.org/contest-dataset>. Moreover, the results presented here can be reproduced by exploiting the code published at <https://github.com/anthonyesp/neurofeedback>.

Acknowledgment

The Authors thank Emanuele Cirillo, Stefania Di Rienzo e Bianca Sorvillo for their precious help in carrying on the experimental campaign. A special thanks goes also to all the volunteers who took part in the experiments.

1. Zampolini, M.; Todeschini, E.; Hermens, H.; Ilsbrouckx, S.; Macellari, V.; Magni, R.; Rogante, M.; Vollenbroek, M.; Giacomozzi, C.; et al. Tele-rehabilitation: present and future. *Annali dell'Istituto superiore di sanita* **2008**, *44*, 125–134.
2. Piron, L.; Tonin, P.; Trivello, E.; Battistin, L.; Dam, M. Motor tele-rehabilitation in post-stroke patients. *Medical informatics and the Internet in medicine* **2004**, *29*, 119–125.
3. Schröder, J.; Van Crielinge, T.; Embrechts, E.; Celis, X.; Van Schuppen, J.; Truijten, S.; Saeys, W. Combining the benefits of tele-rehabilitation and virtual reality-based balance training: a sys-

- tematic review on feasibility and effectiveness. *Disability and Rehabilitation: Assistive Technology* **2019**, *14*, 2–11. 497
4. Coccia, A.; Amitrano, F.; Donisi, L.; Cesarelli, G.; Pagano, G.; Cesarelli, M.; D’Addio, G. Design and validation of an e-textile-based wearable system for remote health monitoring. *Acta Imeko* **2021**, *10*, 220–229. 498–500
 5. Cipresso, P.; Serino, S.; Borghesi, F.; Tartarisco, G.; Riva, G.; Pioggia, G.; Gaggioli, A.; et al. Continuous measurement of stress levels in naturalistic settings using heart rate variability: An experience-sampling study driving a machine learning approach. *ACTA IMEKO* **2021**, *10*, 239–248. 501–505
 6. Mbunge, E.; Muchemwa, B.; Batani, J.; et al. Sensors and healthcare 5.0: transformative shift in virtual care through emerging digital health technologies. *Global Health Journal* **2021**, *5*, 169–177. 506–508
 7. Bulc, V.; Hart, B.; Hannah, M.; Hrovatin, B. Society 5.0 and a Human Centred Health Care. In *Medicine-Based Informatics and Engineering*; Springer, 2022; pp. 147–177. 509–510
 8. Bacanoiu, M.V.; Danoiu, M. New Strategies to Improve the Quality of Life for Normal Aging versus Pathological Aging. *Journal of Clinical Medicine* **2022**, *11*, 4207. 511–512
 9. Truijen, S.; Abdullahi, A.; Bijsterbosch, D.; van Zoest, E.; Conijn, M.; Wang, Y.; Struyf, N.; Saeys, W. Effect of home-based virtual reality training and telerehabilitation on balance in individuals with Parkinson disease, multiple sclerosis, and stroke: a systematic review and meta-analysis. *Neurological Sciences* **2022**, pp. 1–12. 513–516
 10. Belotti, N.; Bonfanti, S.; Locatelli, A.; Rota, L.; Ghidotti, A.; Vitali, A. A Tele-Rehabilitation Platform for Shoulder Motor Function Recovery Using Serious Games and an Azure Kinect Device. In *dHealth 2022*; IOS Press, 2022; pp. 145–152. 517–519
 11. Mansour, S.; Ang, K.K.; Nair, K.P.; Phua, K.S.; Arvaneh, M. Efficacy of Brain–Computer Interface and the Impact of Its Design Characteristics on Poststroke Upper-limb Rehabilitation: A Systematic Review and Meta-analysis of Randomized Controlled Trials. *Clinical EEG and neuroscience* **2022**, *53*, 79–90. 520–523
 12. Padfield, N.; Camilleri, K.; Camilleri, T.; Fabri, S.; Bugeja, M. A Comprehensive Review of Endogenous EEG-Based BCIs for Dynamic Device Control. *Sensors* **2022**, *22*, 5802. 524–525
 13. Prasad, G.; Herman, P.; Coyle, D.; McDonough, S.; Crosbie, J. Applying a brain-computer interface to support motor imagery practice in people with stroke for upper limb recovery: a feasibility study. *Journal of neuroengineering and rehabilitation* **2010**, *7*, 1–17. 526–528
 14. Wen, D.; Fan, Y.; Hsu, S.H.; Xu, J.; Zhou, Y.; Tao, J.; Lan, X.; Li, F. Combining brain–computer interface and virtual reality for rehabilitation in neurological diseases: A narrative review. *Annals of physical and rehabilitation medicine* **2021**, *64*, 101404. 529–531
 15. Wang, Z.; Zhou, Y.; Chen, L.; Gu, B.; Liu, S.; Xu, M.; Qi, H.; He, F.; Ming, D. A BCI based visual-haptic neurofeedback training improves cortical activations and classification performance during motor imagery. *Journal of neural engineering* **2019**, *16*, 066012. 532–534
 16. Arpaia, P.; Coyle, D.; Donnarumma, F.; Esposito, A.; Natalizio, A.; Parvis, M. Visual and haptic feedback in detecting motor imagery within a wearable brain-computer interface. *Measurement* **2022**, p. 112304. 535–537
 17. Singh, A.; Hussain, A.A.; Lal, S.; Guesgen, H.W. A comprehensive review on critical issues and possible solutions of motor imagery based electroencephalography brain-computer interface. *Sensors* **2021**, *21*, 2173. 538–540
 18. Arpaia, P.; Callegaro, L.; Cultrera, A.; Esposito, A.; Ortolano, M. Metrological characterization of consumer-grade equipment for wearable brain–computer interfaces and extended reality. *IEEE Transactions on Instrumentation and Measurement* **2021**, *71*, 1–9. 541–543
 19. Moioli, R.C.; Nardelli, P.H.; Barros, M.T.; Saad, W.; Hekmatmanesh, A.; Silva, P.E.G.; de Sena, A.S.; Dzaferagic, M.; Siljak, H.; Van Leekwijck, W.; et al. Neurosciences and wireless networks: The potential of brain-type communications and their applications. *IEEE Communications Surveys & Tutorials* **2021**, *23*, 1599–1621. 544–547
 20. Teplan, M.; et al. Fundamentals of EEG measurement. *Measurement science review* **2002**, *2*, 1–11. 548
 21. Ienca, M.; Haselager, P.; Emanuel, E.J. Brain leaks and consumer neurotechnology. *Nature biotechnology* **2018**, *36*, 805–810. 549–550
 22. Affanni, A.; Aminosharieh Najafi, T.; Guerci, S. Development of an eeg headband for stress measurement on driving simulators. *Sensors* **2022**, *22*, 1785. 551–552
 23. Arpaia, P.; Callegaro, L.; Cultrera, A.; Esposito, A.; Ortolano, M. Metrological characterization of a low-cost electroencephalograph for wearable neural interfaces in industry 4.0 applications. 553–554

- In Proceedings of the 2021 IEEE International Workshop on Metrology for Industry 4.0 & IoT (MetroInd4.0&IoT). IEEE, 2021, pp. 1–5.
24. Jeong, J.H.; Choi, J.H.; Kim, K.T.; Lee, S.J.; Kim, D.J.; Kim, H.M. Multi-domain convolutional neural networks for lower-limb motor imagery using dry vs. wet electrodes. *Sensors* **2021**, *21*, 6672.
 25. Wang, F.; Li, G.; Chen, J.; Duan, Y.; Zhang, D. Novel semi-dry electrodes for brain–computer interface applications. *Journal of neural engineering* **2016**, *13*, 046021.
 26. Hinrichs, H.; Scholz, M.; Baum, A.K.; Kam, J.W.; Knight, R.T.; Heinze, H.J. Comparison between a wireless dry electrode EEG system with a conventional wired wet electrode EEG system for clinical applications. *Scientific reports* **2020**, *10*, 1–14.
 27. Zhang, Y.; Zhang, X.; Sun, H.; Fan, Z.; Zhong, X. Portable brain-computer interface based on novel convolutional neural network. *Computers in biology and medicine* **2019**, *107*, 248–256.
 28. Lin, B.S.; Pan, J.S.; Chu, T.Y.; Lin, B.S. Development of a wearable motor-imagery-based brain–computer interface. *Journal of medical systems* **2016**, *40*, 1–8.
 29. Lo, C.C.; Chien, T.Y.; Chen, Y.C.; Tsai, S.H.; Fang, W.C.; Lin, B.S. A wearable channel selection-based brain-computer interface for motor imagery detection. *Sensors* **2016**, *16*, 213.
 30. Lisi, G.; Hamaya, M.; Noda, T.; Morimoto, J. Dry-wireless EEG and asynchronous adaptive feature extraction towards a plug-and-play co-adaptive brain robot interface. In Proceedings of the 2016 IEEE International Conference on Robotics and Automation (ICRA). IEEE, 2016, pp. 959–966.
 31. Lisi, G.; Rivela, D.; Takai, A.; Morimoto, J. Markov switching model for quick detection of event related desynchronization in EEG. *Frontiers in neuroscience* **2018**, *12*, 24.
 32. Casso, M.I.; Jeunet, C.; Roy, R.N. Heading for motor imagery brain-computer interfaces (MI-BCIs) usable out-of-the-lab: Impact of dry electrode setup on classification accuracy. In Proceedings of the 2021 10th International IEEE/EMBS Conference on Neural Engineering (NER). IEEE, 2021, pp. 690–693.
 33. Simon, C.; Ruddy, K.L. A wireless, wearable Brain-Computer Interface for neurorehabilitation at home; A feasibility study. In Proceedings of the 2022 10th International Winter Conference on Brain-Computer Interface (BCI). IEEE, 2022, pp. 1–6.
 34. Arpaia, P.; Coyle, D.; Donnarumma, F.; Esposito, A.; Natalizio, A.; Parvis, M.; Pesola, M.; Vallefucio, E. Multimodal Feedback in Assisting a Wearable Brain-Computer Interface Based on Motor Imagery. In Proceedings of the 2022 IEEE International Conference on Metrology for Extended Reality, Artificial Intelligence and Neural Engineering (MetroXRINE). IEEE, 2022, pp. 691–696.
 35. Hekmatmanesh, A.; Nardelli, P.H.; Handroos, H. Review of the state-of-the-art of brain-controlled vehicles. *IEEE Access* **2021**, *9*, 110173–110193.
 36. Ang, K.K.; Chin, Z.Y.; Wang, C.; Guan, C.; Zhang, H. Filter bank common spatial pattern algorithm on BCI competition IV datasets 2a and 2b. *Frontiers in neuroscience* **2012**, *6*, 39.
 37. Arpaia, P.; Esposito, A.; Natalizio, A.; Parvis, M. How to successfully classify EEG in motor imagery BCI: a metrological analysis of the state of the art. *Journal of Neural Engineering* **2022**.
 38. Mullen, T.R.; Kothe, C.A.; Chi, Y.M.; Ojeda, A.; Kerth, T.; Makeig, S.; Jung, T.P.; Cauwenberghs, G. Real-time neuroimaging and cognitive monitoring using wearable dry EEG. *IEEE Transactions on Biomedical Engineering* **2015**, *62*, 2553–2567.
 39. Arpaia, P.; De Benedetto, E.; Esposito, A.; Natalizio, A.; Parvis, M.; Pesola, M. Comparing artifact removal techniques for daily-life electroencephalography with few channels. In Proceedings of the 2022 IEEE International Symposium on Medical Measurements and Applications (MeMeA). IEEE, 2022, pp. 1–6.
 40. Delorme, A.; Makeig, S. EEGLAB: an open source toolbox for analysis of single-trial EEG dynamics including independent component analysis. *Journal of neuroscience methods* **2004**, *134*, 9–21.
 41. Williams, S.E.; Cumming, J.; Ntoumanis, N.; Nordin-Bates, S.M.; Ramsey, R.; Hall, C. Further validation and development of the movement imagery questionnaire. *Journal of sport and exercise psychology* **2012**, *34*, 621–646.
 42. Hall, C.R.; Pongrac, J. *Movement imagery: questionnaire*; University of Western Ontario Faculty of Physical Education, 1983.
 43. Hall, C.R.; Martin, K.A. Measuring movement imagery abilities: a revision of the movement imagery questionnaire. *Journal of mental imagery* **1997**.
 44. Brooke, J.; et al. SUS-A quick and dirty usability scale. *Usability evaluation in industry* **1996**, *189*, 4–7.

45. Bangor, A.; Kortum, P.; Miller, J. Determining what individual SUS scores mean: Adding an adjective rating scale. *Journal of usability studies* **2009**, *4*, 114–123. 614
46. Bangor, A.; Kortum, P.T.; Miller, J.T. An empirical evaluation of the system usability scale. *Intl. Journal of Human–Computer Interaction* **2008**, *24*, 574–594. 615
47. Hart, S.G.; Staveland, L.E. Development of NASA-TLX (Task Load Index): Results of empirical and theoretical research. In *Advances in psychology*; Elsevier, 1988; Vol. 52, pp. 139–183. 618
48. Hart, S.G. NASA-task load index (NASA-TLX); 20 years later. In Proceedings of the Proceedings of the human factors and ergonomics society annual meeting. Sage publications Sage CA: Los Angeles, CA, 2006, Vol. 50, pp. 904–908. 619
49. Schrepp, M.; Hinderks, A.; Thomaschewski, J. Design and evaluation of a short version of the user experience questionnaire (UEQ-S). *International Journal of Interactive Multimedia and Artificial Intelligence*, *4* (6), 103–108. **2017**. 620
50. Cho, H.; Ahn, M.; Ahn, S.; Kwon, M.; Jun, S.C. EEG datasets for motor imagery brain–computer interface. *GigaScience* **2017**, *6*, gix034. 621
51. Rosner, B. *Fundamentals of biostatistics*; Cengage learning, 2015. 622
52. Combrisson, E.; Jerbi, K. Exceeding chance level by chance: The caveat of theoretical chance levels in brain signal classification and statistical assessment of decoding accuracy. *Journal of neuroscience methods* **2015**, *250*, 126–136. 623
53. Batula, A.M.; Mark, J.A.; Kim, Y.E.; Ayaz, H. Comparison of brain activation during motor imagery and motor movement using fNIRS. *Computational intelligence and neuroscience* **2017**, 2017. 624
54. Arpaia, P.; Donnarumma, F.; Esposito, A.; Parvis, M. Channel selection for optimal EEG measurement in motor imagery-based brain-computer interfaces. *International journal of neural systems* **2021**, *31*, 2150003. 625
55. López-Larraz, E.; Montesano, L.; Gil-Agudo, Á.; Minguez, J.; Oliviero, A. Evolution of EEG motor rhythms after spinal cord injury: a longitudinal study. *PloS one* **2015**, *10*, e0131759. 626
56. Lee, D.; Hwang, S. Motor imagery on upper extremity function for persons with stroke: a systematic review and meta-analysis. *Physical Therapy Rehabilitation Science* **2019**, *8*, 52–59. 627
57. De Vries, S.; Tepper, M.; Feenstra, W.; Oosterveld, H.; Boonstra, A.M.; Otten, B. Motor imagery ability in stroke patients: the relationship between implicit and explicit motor imagery measures. *Frontiers in human neuroscience* **2013**, *7*, 790. 628
58. Szameitat, A.J.; Shen, S.; Conforto, A.; Sterr, A. Cortical activation during executed, imagined, observed, and passive wrist movements in healthy volunteers and stroke patients. *Neuroimage* **2012**, *62*, 266–280. 629
59. Bacanoiu, M.V.; Mititelu, R.R.; Danoiu, M.; Oлару, G.; Buga, A.M. Functional recovery in Parkinsons Disease: current state and future perspective. *Journal of Clinical Medicine* **2020**, *9*, 3413. 630
60. Caligiore, D.; Mustile, M.; Spalletta, G.; Baldassarre, G. Action observation and motor imagery for rehabilitation in Parkinson’s disease: A systematic review and an integrative hypothesis. *Neuroscience & Biobehavioral Reviews* **2017**, *72*, 210–222. 631
61. Baniqued, P.D.E.; Stanyer, E.C.; Awais, M.; Alazmani, A.; Jackson, A.E.; Mon-Williams, M.A.; Mushtaq, F.; Holt, R.J. Brain–computer interface robotics for hand rehabilitation after stroke: A systematic review. *Journal of neuroengineering and rehabilitation* **2021**, *18*, 1–25. 632
62. Mladenović, J.; Frey, J.; Pramij, S.; Mattout, J.; Lotte, F. Towards identifying optimal biased feedback for various user states and traits in motor imagery BCI. *IEEE Transactions on Biomedical Engineering* **2021**, *69*, 1101–1110. 633
63. Tao, L.; Cao, T.; Wang, Q.; Liu, D.; Sun, J. Distribution Adaptation and Classification Framework Based on Multiple Kernel Learning for Motor Imagery BCI Illiteracy. *Sensors* **2022**, *22*, 6572. 634
64. Brunner, I.; Lundquist, C.B.; Pedersen, A.R.; Spaich, E.; Dosen, S.; Savic, A. Brain Computer Interface training for patients with severe upper limb paresis after stroke–A randomized controlled pilot trial **2023**. 635